

NAVAL POSTGRADUATE SCHOOL Monterey, California



THESIS

CASIMIR ACOUSTICS

by

Robert Tayag Susbilla

December, 1996

Thesis Advisor:
Co-Advisor:

Andrés Larraza
Bruce C. Denardo

19970623 297

Approved for public release; distribution is unlimited.

DTIC QUALITY INSPECTED 4

REPORT DOCUMENTATION PAGE

Form Approved OMB No. 0704-0188

Public reporting burden for this collection of information is estimated to average 1 hour per response, including the time for reviewing instruction, searching existing data sources, gathering and maintaining the data needed, and completing and reviewing the collection of information. Send comments regarding this burden estimate or any other aspect of this collection of information, including suggestions for reducing this burden, to Washington Headquarters Services, Directorate for Information Operations and Reports, 1215 Jefferson Davis Highway, Suite 1204, Arlington, VA 22202-4302, and to the Office of Management and Budget, Paperwork Reduction Project (0704-0188) Washington DC 20503.

1. AGENCY USE ONLY (Leave blank)	2. REPORT DATE December 1996.	3. REPORT TYPE AND DATES COVERED Master's Thesis	
4. CASIMIR ACOUSTICS		5. FUNDING NUMBERS	
6. AUTHOR(S) Susbilla, Robert T.		8. PERFORMING ORGANIZATION REPORT NUMBER	
7. PERFORMING ORGANIZATION NAME(S) AND ADDRESS(ES) Naval Postgraduate School Monterey CA 93943-5000		10. SPONSORING/MONITORING AGENCY REPORT NUMBER	
9. SPONSORING/MONITORING AGENCY NAME(S) AND ADDRESS(ES)		11. SUPPLEMENTARY NOTES The views expressed in this thesis are those of the author and do not reflect the official policy or position of the Department of Defense or the U.S. Government.	
12a. DISTRIBUTION/AVAILABILITY STATEMENT Approved for public release; distribution is unlimited.		12b. DISTRIBUTION CODE	
13. ABSTRACT (maximum 200 words) When the indirect manifestations of the electromagnetic ZPF are interpreted as due to radiation pressure, acoustic noise can render an excellent analog to probe previous as well as recently proposed behavior. An acoustic chamber for isotropic and homogeneous acoustic noise of controllable spectral shape has been built. The noise can be driven up to levels of 130 dB (re 20 μ Pa) in a band of frequencies up to 50 kHz wide. When driving the system with broadband noise, it will be used (i) to test the Galilean invariance of a spectral shape proportional to the square of the frequency, (ii) the force of attraction between parallel plates (analog to Casimir force), (iii) the acoustic radiation emitted by a cavity that is made to oscillate at high frequencies (analog to the proposed Casimir radiation), (iv) the change in the frequency of oscillation of a pendulum as the noise intensity is varied (analog to the proposed origin of inertia), and (v) the force of attraction between two spheres due to the acoustic shadow that each one casts onto the other (analog to van der Waals force and the proposed origin of gravitation).			
14. SUBJECT TERMS: Casimir Acoustics - Analog to Zero Point Field (ZPF).		15. NUMBER OF PAGES 40	
		16. PRICE CODE	
17. SECURITY CLASSIFICATION OF REPORT Unclassified	18. SECURITY CLASSIFICATION OF THIS PAGE Unclassified	19. SECURITY CLASSIFICATION OF ABSTRACT Unclassified	20. LIMITATION OF ABSTRACT UL

Approved for public release; distribution is unlimited.

CASIMIR ACOUSTICS

Robert T. Susbilla
Lieutenant Commander, United States Navy
B.S., University of Southern California, 1983

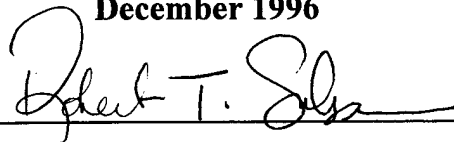
Submitted in partial fulfillment
of the requirements for the degree of

**MASTER OF SCIENCE IN
APPLIED PHYSICS**
from the

NAVAL POSTGRADUATE SCHOOL

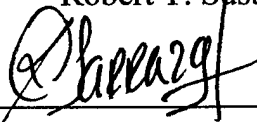
December 1996

Author:



Robert T. Susbilla

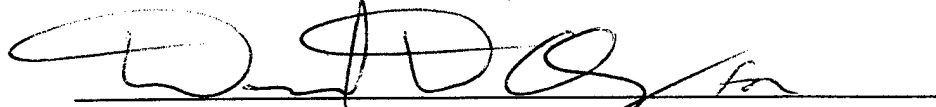
Approved by:



Andrés Larraza, Thesis Advisor



Bruce C. Denardo, Co-Thesis Advisor



Anthony A. Atchley, Chairman

Department of Physics

ABSTRACT

When the indirect manifestations of the electromagnetic ZPF are interpreted as due to radiation pressure, acoustic noise can render an excellent analog to probe previous as well as recently proposed behavior. An acoustic chamber for isotropic and homogeneous acoustic noise of controllable spectral shape has been built. The noise can be driven up to levels of 130dB (re 20 μ Pa) in a band of frequencies up to 50 kHz wide. When driving the system with broadband noise, it will be used (i) to test the Galilean invariance of a spectral shape proportional to the square of the frequency, (ii) the force of attraction between parallel plates (analog to Casimir force), (iii) the acoustic radiation emitted by a cavity that is made to oscillate at high frequencies (analog to the proposed Casimir radiation), (iv) the change in the frequency of oscillation of a pendulum as the noise intensity is varied (analog to the proposed origin of inertia), and (v) the force of attraction between two spheres due to the acoustic shadow that each one casts onto the other (analog to van der Waals force and the proposed origin of gravitation).

TABLE OF CONTENTS

I. INTRODUCTION.....	1
II. APPARATUS	9
A. REQUIREMENTS FOR THE EXPERIMENTS.....	9
1. Conditions.....	9
2. Limitations	10
B. ACOUSTIC CHAMBER DESIGN AND CONSTRUCTION.....	11
1. Cylinder	11
2. Signal Sensing.....	12
C. DRIVER SELECTION	13
D. EXPERIMENTAL RESULTS	17
1. Verification of Conditions.....	17
2. Casimir Force Experiment	20
III. PROPOSED EXPERIMENTS AND CONCLUSIONS.....	23
A. ACOUSTIC ANALOG TO THE CASIMIR EFFECT.....	23
B. ACOUSTIC ANALOG TO THE PROPOSED ORIGIN OF INERTIA.....	26
C. CONCLUSIONS.....	27
LIST OF REFERENCES	29
INITIAL DISTRIBUTION LIST.....	31

I. INTRODUCTION

According to quantum field theory, the vacuum state of the electromagnetic field has zero expectation value because it is a state of no real photons. However, the square fluctuations of the electromagnetic field are infinite because each classical normal mode of frequency ω has an associated quantum zero-point energy $\frac{1}{2}\hbar\omega$. Thus, the vacuum state is a state where the electromagnetic energy is infinite but no electromagnetic fields are present. Although the electromagnetic zero-point field (ZPF) cannot be measured directly, its effects are manifested in a variety of phenomena, including the Casimir force (Casimir, 1948), the van der Waals force between polarizable matter (Casimir and Polder, 1948), spontaneous emission of radiation, and the Lamb shift (Sakurai, 1967).

In the Casimir effect, two uncharged conducting parallel plates alter the mode structure of the ZPF in free space, resulting in an attractive force. The difference between the vacuum electromagnetic energy for infinite plate separation and a finite plate separation is the interaction energy between the plates, from which the force is calculated. If the plates are a distance d apart, the force per unit area is proportional to $\hbar c/d^4$. Although this result can be proven rigorously, it can be shown by dimensional analysis that this is the only possible combination in which \hbar , c , and d can be united to yield a force per unit area. The constant of proportionality is a pure number, and a rigorous

calculation yields the value $\pi^2/240$.

Physically, the electromagnetic ZPF fluctuations induce local dipoles in both plates and because of the spatial correlations of the fluctuations the interaction of these dipoles leads to a net attractive force. Based on this argument, there must also be a Casimir force between two parallel dielectric plates (Lifshitz, 1956 and Schwinger et al., 1978).

At present, only a qualitative experimental verification of the Casimir effect has been made (Sparnaay, 1958). Casimir and Polder (1948) have shown that polarizable matter also alters the mode structure of the ZPF. The resulting force of attraction is the van der Waals force. Experiments (Sukenic et al., 1993) that measure the deflections of ground-state sodium atoms passing through a micro-sized parallel plate cavity have provided clear evidence for the existence of the Casimir-Polder force.

Recently, two new results have been obtained from the properties of the ZPF. In the first of these results, Schwinger (1993) and Eberlein (1996), in an attempt to explain the emission of light from a collapsing bubble (sonoluminescence), have predicted that the accelerated walls of a dielectric cavity would emit non-dipolar broad-band light due to non-adiabatic changes of the volume. Physically, because the electromagnetic ZPF excites fluctuating dipoles on the stationary surface of a dielectric discontinuity (a mirror), virtual two-photon states are perpetually excited by the mirror in the vacuum. However, the fluctuating forces on either side of the mirror are balanced against each other, so that no mean radiation pressure acts on the mirror. Because of

Lorentz invariance, a mirror moving with constant velocity would not experience any mean radiation pressure either. However, when the mirror accelerates the fluctuating dipoles become a source of radiation. For sonoluminescent bubbles, the peak acceleration at the minimum radius is calculated to be about 13 Tera g's with a turnaround time of 10 ps. Even if this "Casimir radiation" mechanism does not adequately explain sonoluminescence, it should be tested experimentally.

In the second recent result using the properties of the ZPF, Haisch, Rueda, and Puthoff (1994) have put forward the proposal that inertia, and hence Newton's second law, can be *derived* from first principles in terms of the ZPF. Because gravitational mass and inertial mass are equivalent, this idea would make gravitation an electromagnetic effect.

This thesis deals with an apparatus for experimental investigations of what we call *Casimir acoustics*. The central feature of this new area of basic research is that it can test, by analogy, certain aspects of the ZPF that would be very difficult or impossible to verify directly by experiments. A simplified point of view of the ZPF is that it is merely a very broad-band noise of some specific spectral shape ($4\pi\hbar\omega^3/c^3$). An advantage of acoustics is that we can control not only the shape of the spectrum, but also the intensity.

We can consider measurements of the force of attraction between two plates of a given acoustic impedance, and find the dependence on the separation distance for different spectral shapes of the noise. This would provide the acoustic analog to the Casimir and the Casimir-Polder forces. This

analogy follows because the attraction between two plates can also be understood superficially, in terms of the radiation pressure exerted by plane waves of some spectral shape distributed isotropically in space. In the space between the plates, the modes formed by reflections off the plates act to push the plates apart. The modes outside the resonant cavity formed by the plates act to push the plates together. For the electromagnetic ZPF, both the total outward pressure and the total inward pressure are infinite, but it is only the difference that is physically meaningful. This difference leads to an attractive force because the modes in the space outside the plates form a continuum, whereas those inside are restricted to discrete values of the component of the wavevector perpendicular to the plates. There are “more” modes outside to push the plates together by radiation pressure than there are modes between the plates to push them apart.

If we consider rigid plates of very large acoustic impedance, for a spectral energy of the form $A\omega^\beta$, where A and β are constants, dimensional analysis reveals that the only possible combination in which A , c (the speed of sound), and d can be united to yield a force per unit area is of the form

$$Ac^{\beta+1}/d^{\beta+1}. \tag{1.1}$$

The ZPF is homogeneous and isotropic (it looks the same in all points of space and time, and in all directions). It is also Lorentz invariant (any two inertial observers do not see a difference). One can say that the ZPF is

undetectable in any inertial frame because homogeneity, isotropy, and Lorentz invariance do not allow an observer to see any contrast between directions, times, and inertial frames. A Lorentz transformation Doppler shifts the frequency and also alters the intensity of radiation. The only spectral shape that is the same for any inertial frame is proportional to the cube of the frequency (Boyer, 1969).

A sound field requires a fluid as a medium. In this case, the fluid equations of motion are invariant under Galilean transformations. In a similar way as a Lorentz transformation, a Galilean transformation Doppler shifts the sound frequency and also alters the intensity of the acoustic field. For a spectrum to be Galilean invariant for all inertial frames in the fluid, its spectral shape must be proportional to the square of the frequency. Unlike the ZPF, this Galilean invariant spectral shape can be tested experimentally by using a microphone moving at constant velocity and measuring the spectrum. Different spectral shapes can also be tested not to be Galilean invariant.

The acoustic analog to Casimir radiation can be explored by constructing a cavity with a finite acoustic impedance discontinuity immersed in a medium with broad-band noise. If the cavity is made to oscillate at a very large frequency, what is the spectrum of acoustic emission? Due to the presence of the acoustic noise background, the emission should be a broadband spectrum different from the background because the boundary is accelerating. In contrast to the electromagnetic case, the acoustic analog of Casimir radiation is readily testable because the time scales involved are much bigger (by at least 8 orders

of magnitude), and the requisite accelerations much smaller (by about 8 to 16 orders of magnitude).

In another experiment, the effect of broad-band noise on the resonant frequency of an oscillator can be measured. The frequency of oscillation of a mass at the end of a spring is inversely proportional to the square root of the mass. In the presence of a broadband isotropic acoustic noise, the inertial mass of the oscillator will increase due to an effect akin to the Kelvin mass of an accelerated object moving through an ideal fluid. Physically, the accelerated mass distorts the spectrum due to non-inertial Doppler shifts of the frequency and alterations of the spectral acoustic intensity. The mass does work against the background of acoustic noise which in turn opposes these changes.

Preliminary results show that both a resistive inertial force that depends on the instantaneous acceleration and a drag force that depends on the instantaneous velocity will alter the motion of the oscillator. Due to the drag force, the oscillator will suffer an added attenuation. Due to the resistive inertial force, the inertia of the oscillator will effectively increase and the frequency of oscillation will decrease with increasing acoustic intensity. In this case, an acoustic analog to the ZPF origin of inertia can be probed because, in contrast to the electromagnetic ZPF, acoustic noise can be turned off.

Finally, an object placed in an isotropic, homogeneous, broadband acoustic noise does not experience a net force. However, the mass will jiggle in a motion analogous to a *Zitterbewegung*. If a second object is brought into proximity, a force of attraction between two objects will result. This is due to the

acoustic shadow that each one casts onto the other. This proposed experiment then constitutes an acoustic analog to van der Waals force and to the proposed ZPF origin of gravitation.

Casimir acoustics may provide a powerful tool in the understanding of zero point field effects. Our first step is the construction of an acoustic chamber where homogeneous broad-band noise can be driven isotropically in air. Chapter II details the design and construction of such chamber. Preliminary experimental tests of the frequency response of the chamber as well as isotropy of the acoustic noise are also detailed in Chapter II. Proposed experiments and conclusions are presented in Chapter III.

II. APPARATUS

A. REQUIREMENTS FOR THE EXPERIMENTS

The acoustic chamber was designed to perform experiments in Casimir Acoustics that would (i) test the Galilean invariance of a spectrum proportional to ω^2 , (ii) measure the force between two parallel plates due to the radiation pressure of a broadband noise, (iii) measure the broadband radiation of a cavity oscillating at a high frequency while immersed in a medium with broadband noise, and (iv) measure the change of oscillation frequency of an oscillator in broadband acoustic noise. Below, we describe the various tests that we performed to determine whether the chamber was appropriate to conduct all the desired experiments.

1. Conditions

In order to perform these experiments, we must provide a homogeneous and isotropic acoustic field. For a spectrum proportional to ω^2 , these conditions hold true for any inertial frame of reference. The output of a noise source can be filtered to a shape for the desired Galilean invariant acoustic spectrum. These conditions can be established in our acoustic chamber. For instance, the low frequency tail of an RC analog high pass filter has a voltage rolloff proportional to the frequency. If the -3 dB point of the filter is selected at the high frequency rolloff of the drivers, then the resulting spectrum should be proportional to ω^2 .

2. Limitations

The limitations in the four acoustic analogs proposed above are due mainly to the sources for sound. In particular, the typical frequency range limits the possible dimensions of the apparatus if the effects we are seeking are to be observed. For a frequency of 50 kHz, the corresponding wavelength for sound in air is about 7 mm.

For the acoustic analog to the Casimir effect, it is important to have several modes within the plates and hence a sufficiently large separation between them. On the other hand, for a positive value of the exponent β in the spectrum (1.1), the force decreases with distance. When the acoustic noise intensity level is 120 dB, for a plate separation of 5 cm and plate dimensions of 20 cm by 20 cm, the estimated force of attraction between plates is of the order of 0.1 mN.

The acoustic analogs to inertia and Casimir radiation require the dimensions of oscillator and cavity, respectively, to be large compared to the wavelength. Except for numerical factors, for a sphere of volume V undergoing oscillations the added inertia is of the form VE/c^2 where E is the acoustic energy density and c is the speed of sound. Using light spheres (such as Christmas or ping-pong balls) the mass correction can be a measurable effect, as large as 1% to 2% for a 120 dB noise field for 1 g bob (Larraza, 1996).

B. ACOUSTIC CHAMBER DESIGN AND CONSTRUCTION

1. Cylinder

The chamber used to contain the noise is made from a cylindrical air compressor tank (Fig. 2.1). The cylinder is manufactured from steel with a wall thickness of 0.25 inches. The dimensions are 20 inches in diameter and 48 inches in length. One end is ellipsoidal and the other is open to provide access into the chamber. The irregular geometry is a three dimensional stadium, which prevents acoustic shadows or any acoustic contrast between any region in the chamber. In operation, a 2 inch thick plexi-glass plate is bolted onto the open end to provide an acoustic seal. A wide slit was cut at the top of the cylinder to allow attachment of a seating surface for a slide bar that positions the signal sensing device at almost any point inside the chamber.

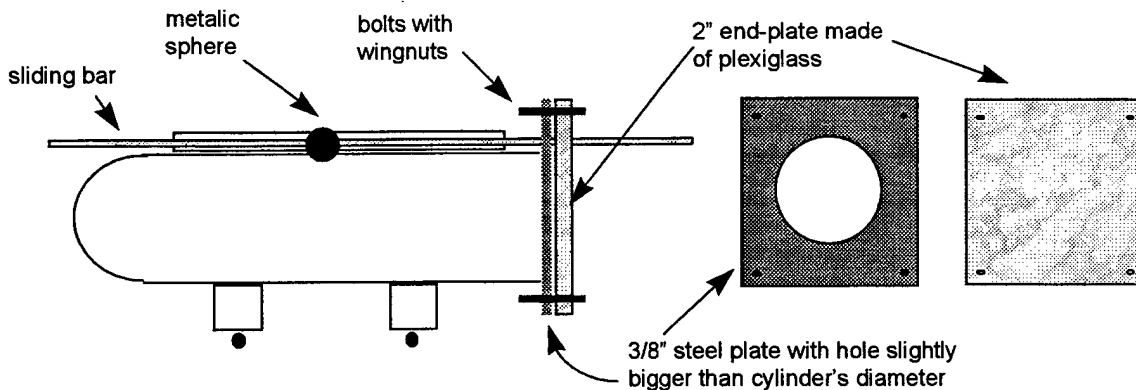


Figure 2.1 Schematic view of the acoustic chamber. The chamber is 48" long, 20" in diameter, and 1/4" thick steel. The microphone probe is mounted on a horizontal sliding bar approximately twice the length of the chamber.

It is desirable to have a rigid cylinder wall to minimize transmission of acoustic energy outside of the tank. The reason is two-fold: to provide hearing

safety, and to maximize the acoustic intensity in the chamber. The 0.25 in. thick steel wall of the cylinder was almost adequate. To further minimize the transmission losses, the Q for flexural modes across the cylinder must be lowered. The cylinder was padded with a pliable sound deadening material that is 0.07 inches thick to further reduce the sound pressure levels outside the chamber. Other improvements can be done to lower the Q for flexural modes, such as providing an aluminum jacket around the chamber, installing metal staves axially along the cylinder or covering the cylinder with aluminum tape. It is also important that the acoustic chamber is air-tight. We found that the end plate and horizontal sliding bar had to be securely clamped to minimize leakage. Clamping provided an improvement of 0.2 dB in total acoustic power.

2. Signal Sensing

In order to verify that the acoustic field is homogeneous and isotropic, we must be capable of measuring the acoustic field everywhere inside the chamber. To perform subsequent experiments without any interruption, we designed a signal sensing device that would provide the capability to measure the acoustic field anywhere inside the acoustic chamber. This was accomplished by using a slide bar/ball arrangement mounted on top of the acoustic chamber as shown in Fig. 2.1. The slide bar is moved axially along the cylinder. Fig. 2.2 is a cross-sectional view of the acoustic chamber. A ball-seat assembly is mounted in the center of the slide bar where the ball is seated in such a way that allows three dimensional movement of a rod threaded through the center of the ball. At the

bottom of the rod is a Larson Davis ¼ inch microphone that has a flat response (± 1 dB up to about 22 kHz and ± 2 dB to 90 kHz). The two movements together provide a way of measuring the acoustic field almost anywhere inside the chamber.

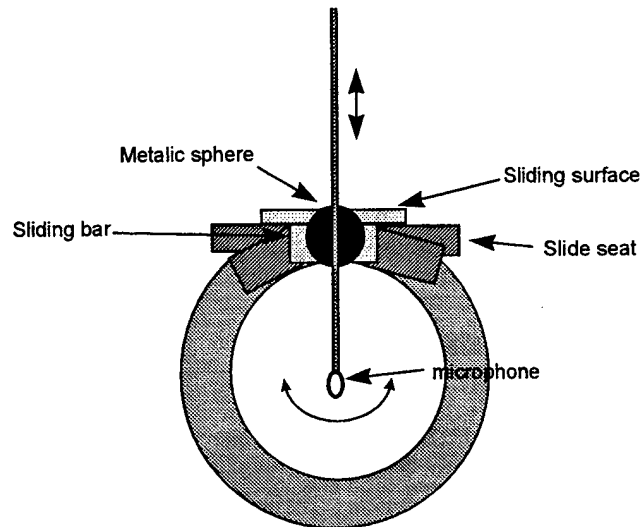


Figure 2.2. Sensing design for acoustic chamber that provides access to nearly every point. The metallic sphere provides azimuthal motion while the bar gives vertical motion. The noise distribution inside the chamber can be probed and the three dimensional isotropy of the noise can be tested. A Larson Davis ¼" microphone is mounted at bottom of probe.

C. DRIVER SELECTION

Using commercial acoustic drivers, we can achieve frequencies as high as 50 kHz. The acoustic spectrum currently covers the range from 0.5 to 50 kHz. For frequencies between 0.5 to 5 kHz, we used a JBL Model 2445J Compression Driver whose frequency response as measured on a terminated tube is within ± 1 dB from 500 Hz to 3.3 kHz, with a 6 dB/octave roll-off above that point. For the frequency range between 5 to 50 kHz, we used the Motorola Direct Radiating Grill piezoelectric tweeter.

Figure 2.3 shows the frequency response of the piezo tweeter in an anechoic chamber using a General Radio Company 1390-B Random Noise Generator as the source. The Random Noise Generator was passed through a 115 dB/octave bandpass filter [Stanford Research Systems (SRS) Model 650] set at a band of 3 kHz to 54 kHz. The output of the filter was then amplified by a Techron 5530 Power Amplifier rated at 310 watts minimum RMS into a 16 ohm load (mono) with flat frequency response (± 0.15 dB) from DC to 200 kHz at 1 watt into 16 ohms. The curve is essentially flat and is considered adequate for the tweeters' intended use.

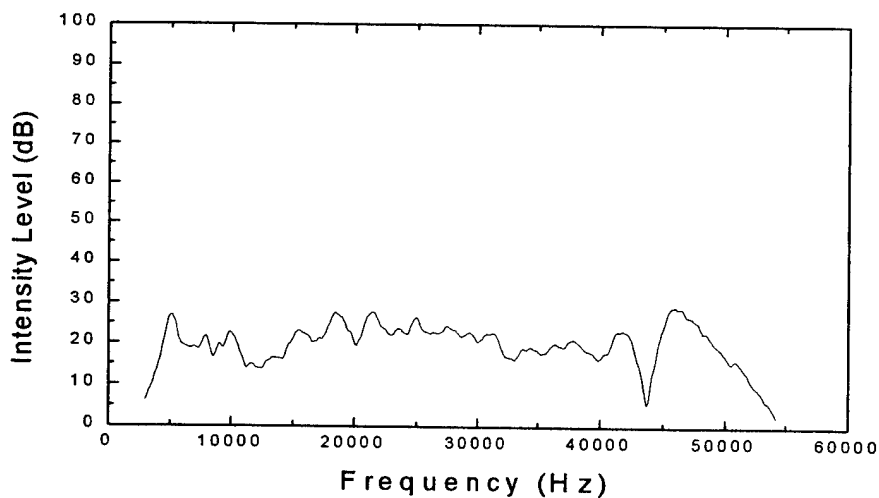


Figure 2.3 Frequency response for the Motorola Piezoelectric Direct Radiating tweeter, Model KSN1078. Measurements were taken at 8 V and at 1 m from the tweeter.

Piezoelectric devices have much higher impedances than conventional acoustic drivers (typically 8 or 16 ohm) but the impedance varies with frequency as shown in Fig. 2.4a. The devices behave as capacitors where the impedance decreases with frequency. Because the bandwidth of the Techron 5530 power

amplifier extends beyond 100 kHz, a 50 ohm (10 watt) resistor was placed in parallel with the tweeter to provide stability by preventing high frequency resonances.

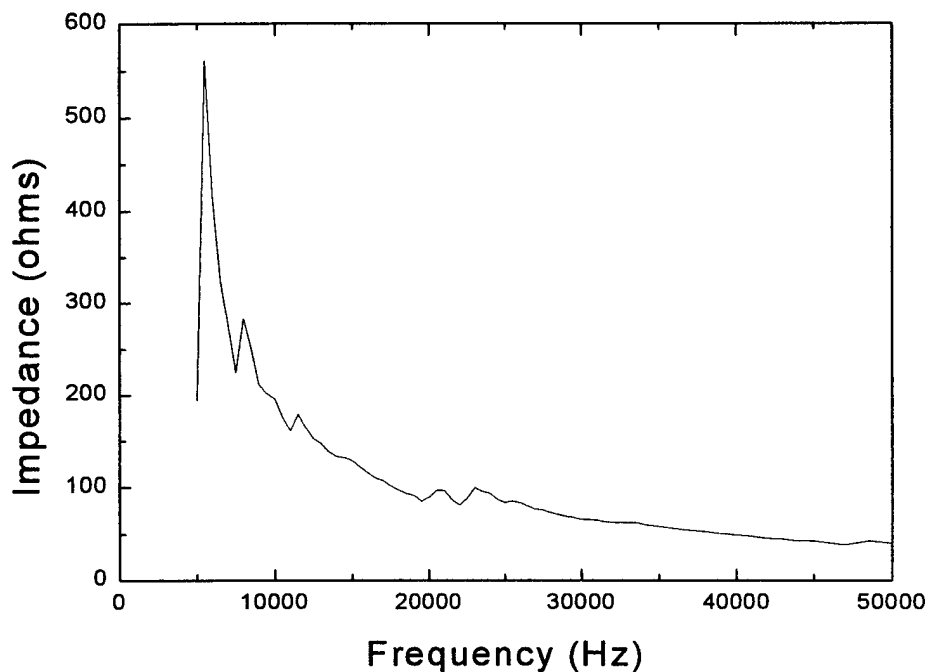


Figure 2.4a Impedance measurement for a single Motorola tweeter using a HP 4194A Impedance/Gain-Phase Analyzer.

Because of the higher impedances, several piezo tweeters in parallel can be driven by a single amplifier without amplifier loading problems. We initially started with 7 piezoelectric drivers, but as seen from Fig. 2.4b, the impedance was reduced dramatically, and was consistently below 3 ohms at frequencies above 11 kHz. This caused loading problems with the amplifiers. Adding a 50 ohm resistor in parallel with the 7 tweeters increased the frequency to above 27 kHz. From our testing we saw that the amplifier was power-limited because of

an overall low impedance of 3 ohms. If a single piezo is driven, the amplifier would be voltage-limited because the amplifier is expecting an 8 ohm load but, in fact, the amplifier sees a variable load with a minimum impedance of about 45 ohms. For enough tweeters in parallel, the amplifier becomes power limited.

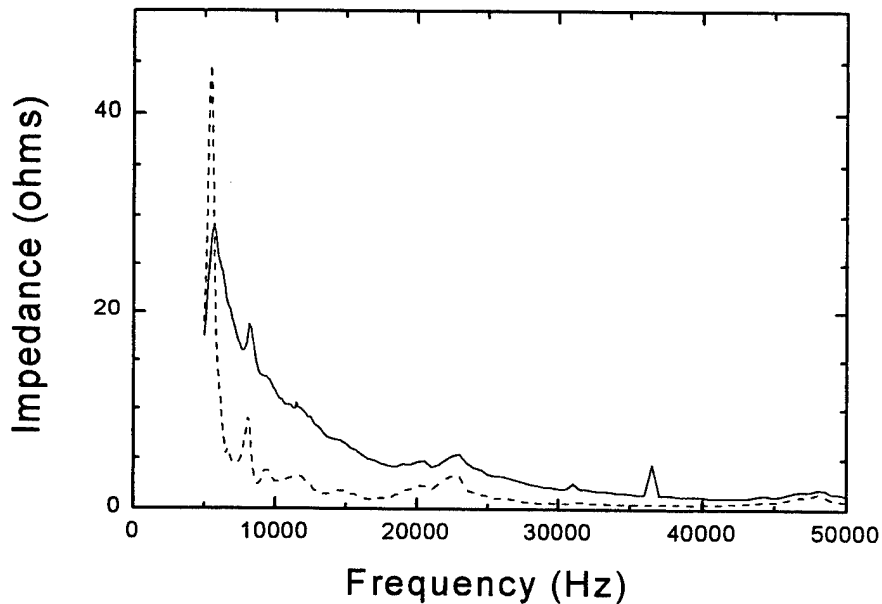


Figure 2.4b Impedance measurement for seven Motorola tweeters in parallel using a HP 4194A Impedance/Gain-Phase Analyzer. The dashed line corresponds to impedance data with a 50 ohm resistor added in parallel.

As shown in Fig. 2.5, we developed an operating curve for one tweeter which indicated that the optimal operating voltage was 12 volts rms. With one 5530 Techron amplifier, we were able to drive 4 Motorola tweeters in parallel at 12 volts without loading problems and yielded a total acoustic power of 122 dB. In fact, the total power increased by 2 dB from a 4 driver to 8 driver configuration with two amplifiers operating at 12 volts. Further setups can be explored such as placing tweeters in series and parallel combinations. The overall impedance

can be adjusted as seen by the amplifier and will thus mitigate loading problems.

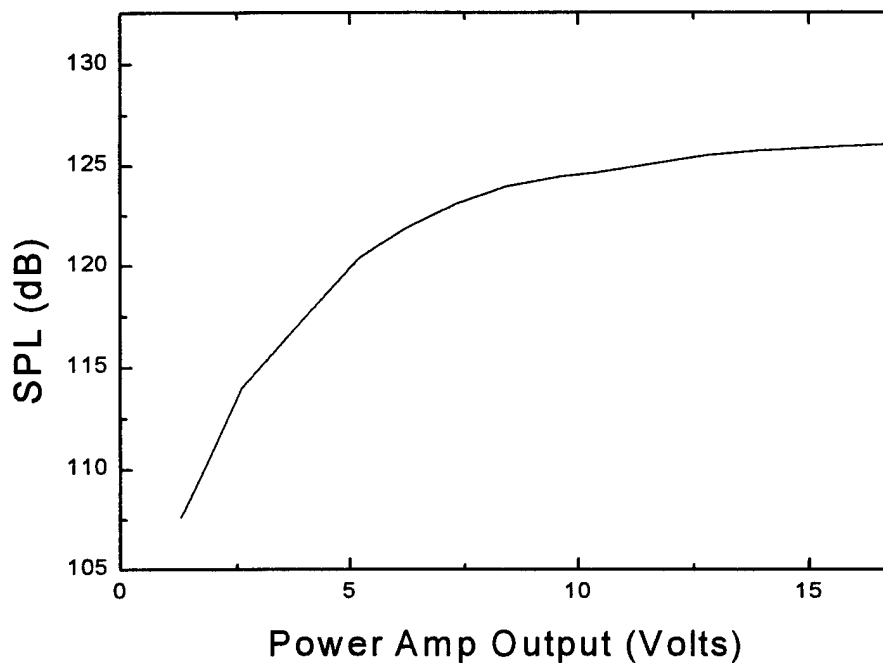


Figure 2.5 Motorola tweeter operating curve. Microphone separation from Motorola driver was approximately 7cm (far field for 5 kHz)

D. EXPERIMENTAL RESULTS

1. Verification of Conditions

Initially, seven Motorola tweeters and a JBL compression driver were placed in the acoustic chamber. The JBL midrange compression driver was placed at the bottom of the chamber on the plexi-glass end. Two slightly opposing piezo tweeters were mounted about midway up the circumference of the chamber at distances of 20-24 cm, 54-60 cm and 83-87 cm from the plexi-glass cover. One additional tweeter was mounted at the ellipsoidal end of the

chamber. Measurements of the acoustic field were taken at distances of 25 cm, 43 cm, 50 cm, 63 cm and 75 cm from the plexi-glass cover. At each distance, the angle of the probe was changed to 150°, 180° and 210° with respect to the horizontal plane (Fig. 2.2), providing a total of 15 locations to measure the acoustic field. The length of the probe in the chamber was constant at all angles measured. The goal was to verify that a homogenous and isotropic acoustic field exists inside the acoustic chamber. A separate 48 dB/octave band pass filter (Krohn-Hite Model 3988) was used for the midrange driver and was powered by a Techron 5507 power amplifier rated at 70 watts minimum RMS (mono) into a 16-ohm load. This amplifier has a flat frequency response (± 0.2 dB) from 20 Hz to 20 kHz at 1 watt into 16 ohms. A separate bandpass filter allowed the flexibility of manipulating the acoustic spectrum shape.

The random noise input into the Motorola tweeters was filtered using a 115 dB/octave bandpass filter [Stanford Research Systems (SRS) Model 650] or a 48 dB/octave band pass filter (Krohn-Hite Model 3988) to yield a 6 kHz to 50 kHz band. This filtering eliminates the peak present around 5 kHz. The HP 35670A Dynamic Signal Analyzer averaged the acoustic field measured in the chamber over time in the same way as was done in the case of measuring the frequency response of the Motorola tweeter using the Random Noise Generator. Figure 2.6 combines the acoustic fields of all 15 locations. The acoustic field is essentially the same at every location sampled and is sloped downward (20 dB) with an average total acoustic power of 123.6 dB.

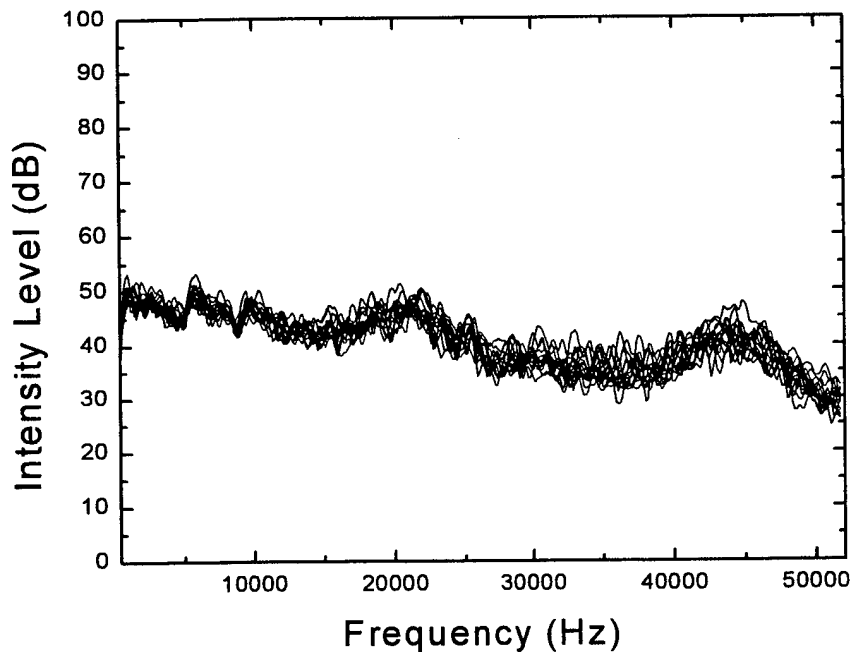


Figure 2.6. Homogeneity and isotropy test using one JBL midrange driver (500 Hz - 20 kHz) and seven Motorola tweeters (5 kHz - 50 kHz). Fifteen locations were sampled, 25 cm, 43 cm, 50 cm, 63 cm, and 75 cm from plexi-glass end. At each location, the probe was positioned at 150°, 180°, and 210° with respect to the top of the chamber.

Another goal was to achieve a total acoustic power of at least 130 dB.

This required 12 tweeters and one midrange driver. The tweeters are driven separately in sets of four. A separate 48 dB/octave band pass filter (Krohn-Hite Model 3988) was used for two tweeter sets. Another noise generator (SRS Model DS 345) was used as the source for this bandpass filter. Measurements of the acoustic field were taken at 25 cm, 43 cm, 50 cm, 75 cm and 100 cm. Angular measurements were also taken yielding a total of 18 sample points. Figure 2.7 combines the acoustic field of all sample points. Again the acoustic field is essentially the same with an average total acoustic power of 133 dB.

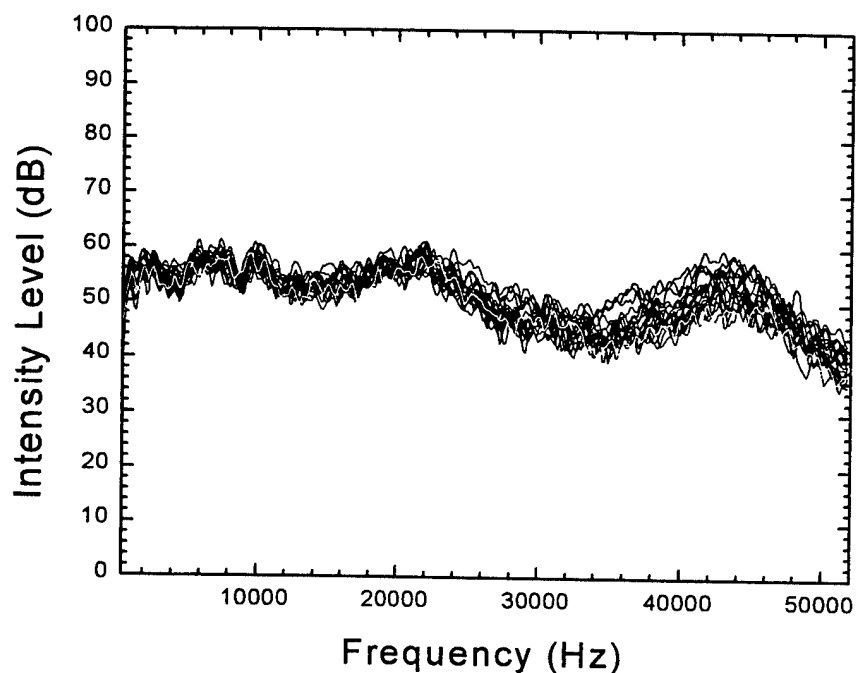


Figure 2.7 Homogeneity and isotropy test using one JBL midrange driver (500 Hz - 20 kHz) and twelve Motorola tweeters (5 kHz - 50 kHz). Eighteen locations were sampled, 25 cm, 43 cm, 50 cm, 63 cm, 75 cm and 100 cm from plexi-glass end. At each location, the probe was positioned at 150°, 180°, and 210° with respect to the top of the chamber.

2. Casimir Force Experiment

The first experiment conducted in the acoustic chamber was the acoustic analog to the Casimir force. The objective of this experiment was to ascertain if the effects of radiation pressure could be visually detected. Figure 2.8 is a representation of the experimental setup. The plates are made of stiff Styrofoam 0.5 inches thick with dimensions 20 cm by 20 cm. Each plate is suspended inside the chamber by two strings of about 10 cm in length. The separation between the plates is about 0.5 cm.

of modes outside > # of mode inside
results in attractive force

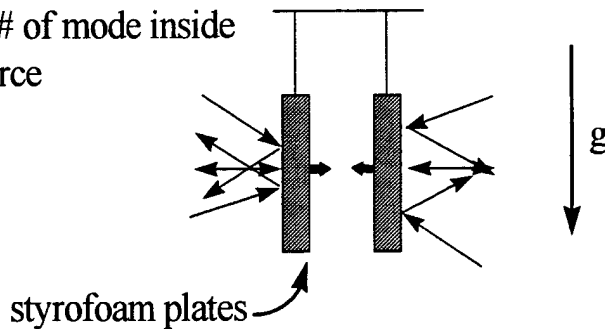


Figure 2.8 Acoustic analog experiment for the Casimir force. The plates are 20 cm by 20 cm and 0.5 inches thick. Plate separation is 0.5 cm.

When the acoustic field is turned on, the radiation pressure from modes inside the cavity formed by the plates will act to push the plates apart. The modes that form inside the cavity depend on the acoustic impedance of the Styrofoam plates ($\approx 2\pi f$) and the separation distance of the plates. A separation of 0.5 cm will only allow those normal modes with a pressure variation across the plate's separation that are above 33.4 kHz. However, low frequency modes with pressure distribution along the plates are possible. The radiation pressure due to modes outside the plates will act to push the plates together. Because only discrete normal modes of frequency exist inside the cavity, there would be more modes outside the cavity and thus the plates would experience an attractive force.

A deflection of the plates due to the radiation pressure was not visually detected. For a 0.5 cm plate separation, the force acting on the plates due to the total radiation pressure was calculated to be about 0.1 mN with an acoustic intensity level at 120 dB (Larraza, 1996). Since each plate mass is 0.04 kg, the

angle of deflection would be 2.5×10^{-4} rad. For a 10 cm string this angle would give a deflection equal to 0.03 mm. The resolving power for a 20/20 vision is about 30 lines per mm at 0.1 m, which explains why visual detection was not apparent.

However, there were some interesting results from the experiment. First, the plates did vibrate. This may have been due to fluctuations of the noise and is thus analogous to the "Zitterbewegung" effect. Second, the intensity levels measured between the plates (132 dB) were higher than what was measured just outside the plates by 5 dB. This should have resulted in a repulsive force.

The acoustic spectrum was incrementally measured in several frequency bands inside and outside the cavity formed by the plates using the Larson Davis ¼" microphone and the HP 35670A Dynamic Signal Analyzer (Swept Sine mode). The separation of the Styrofoam plates was adjusted to 2 cm to allow placement of microphone inside the cavity. Between 1300 Hz and 1400 Hz there were large pressure amplitudes inside the cavity corresponding to the predicted resonances of the first modes of the cavity. Q-amplification of the modes may thus result in higher intensity level inside the cavity.

Qualitative observations indicate that the optimal band that would lead to an attractive force due to radiation pressure is in the band between 6–50 kHz. Also, repulsive force measurements may result for a 1.0-1.3 kHz band.

III. PROPOSED EXPERIMENTS AND CONCLUSIONS

This chapter discusses two proposals for experiments in Casimir acoustics. The first is another attempt to quantify the Casimir effect using an arrangement similar to the Cavendish experiment. The second provides a method to probe the analog to the ZPF effects on inertia.

A. ACOUSTIC ANALOG TO THE CASIMIR EFFECT

As discussed in Chapter II, the initial experimental arrangement to detect the force of attraction between two plates due to radiation pressure may not be sufficiently sensitive. For a 120 dB noise intensity, the estimated angle of deflection for the hanging plates would be 2.5×10^{-4} rad. Thus in the extreme case of a hanging length comparable to the diameter of the chamber, the deflection would be equal to 1 tenth of a millimeter which is at the threshold of sensitivity for visual detection of an adult.

To overcome some of the difficulties inherent to our original arrangement, one could construct an apparatus very similar to the that employed by Cavendish to measure the gravitational constant . With such arrangement, the restoring effects of the weight of the plates are eliminated and the effects of a force between the plates are amplified.

Figure 3.1 shows a schematic of the apparatus. A long monofilament fiber is attached overhead and suspended inside the acoustic chamber. A long

single element fiber is desired in order to minimize the fiber restoring torque due to torsion. On the other end of the fiber is attached a long lightweight rod. A large moment arm yields a greater torque resulting in a greater deflection. Rigid plates are attached on both ends of the rod attached in such way that the center of mass lies under the rod. This is required for stability against rotations about an axis perpendicular to the plane defined by the plates. Two additional plates mounted on stands are placed inside the acoustic chamber and are positioned to oppose the plates mounted on the rods with a separation that can be varied.

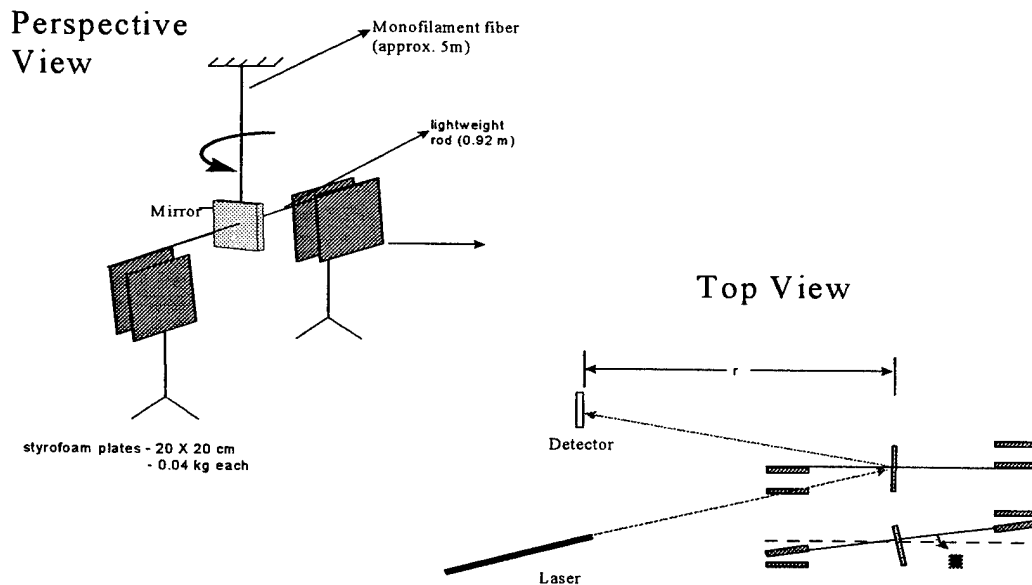


Figure 3.1. Cavendish-type apparatus constructed for a Casimir force experiment using a monofilament fiber attached overhead and suspended inside the acoustic chamber through the center of the metallic sphere. Attached to the fiber is a lightweight rod and on either end are mounted two rigid plates. Two fixed plates mounted on stands inside the acoustic chamber are positioned to oppose the plates mounted on the rod. A laser may be used to measure the deflection of the rod when the plates are subjected to acoustic broadband noise

The amount of rotation can be measured by using a laser (Fig. 3.1, top view). A mirror is attached at the center of the rod where the laser beam is

reflected to a relatively distant scaled detector to record the small deflections. For small angles of deflection θ , the deflection d varies linearly with distance r from the detector to the mirror as $d = r\theta$. Other methods of detection (e.g., inductive) can also be used.

The amount of deflection can be calculated as follows. The torque τ_C due to the Casimir force F_C is

$$\tau_C = F_C L , \quad (3.1)$$

where L is the length of the rod. In equilibrium, τ_C is balanced by the torque due to torsion τ_T :

$$\tau_T = \mu \frac{\pi a^4}{2\ell} \theta , \quad (3.2)$$

where θ is the deflection angle and where we have assumed a cylindrical fiber of radius a , length ℓ , and shear modulus μ . Experimentally, the torsion constant per unit length, $\mu\pi a^4/2$, can be determined by measuring the frequency of oscillation of a torsional pendulum of known moment of inertia. From Eqs (3.1) and (3.2), the angle of deflection is thus

$$\theta = \frac{2F_c L \ell}{\pi \mu a^4} . \quad (3.3)$$

For a 1/50 inch thick, 5 m long, steel fiber (shear modulus about 10^{11} Pa), the deflection angle due to a force of 0.1 mN in a Cavendish balance with an arm of .5 m is 0.4 rad.

B. ACOUSTIC ANALOG TO THE PROPOSED ORIGIN OF INERTIA

A mass m at the end of a spring with spring constant k undergoes simple harmonic motion with angular frequency

$$\omega = \sqrt{\frac{k}{m}} . \quad (3.4)$$

Any change in the frequency of oscillation ω would be due only to modifications of the inertia due to the acoustic field. Because the percentage difference in the inertia depends on the mass of the object, light objects and weak springs must be used.

The frequency of oscillation can be measured inductively by using two coaxial inductors located at the equilibrium point of the object (Fig. 3.2). The object must be a conductor in order for this technique to work. A steady current in one coil will set up a magnetic flux linking the other coil. When the object oscillates about its equilibrium point, an emf appears in the second coil due to the mutual inductance of the two coils. This emf can be displayed on an

oscilloscope and plotted.

This method of measurement can also be implemented in the Cavendish experiment. In this experiment, a conducting plate is installed at the pivot point in lieu of the mirror. The plate is mounted axially along the rod. The two coaxial coils are positioned perpendicular to the plate. When the rod is deflected, the aspect of the plate changes and induces a change in emf on one coil.

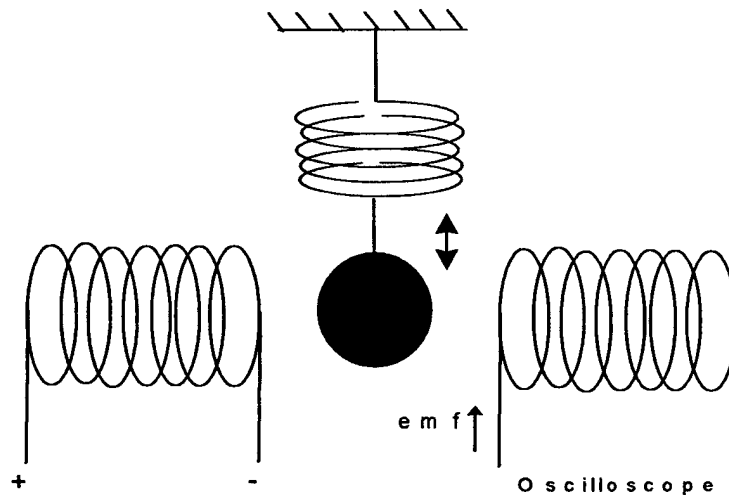


Figure 3.2. Method of measuring frequency of oscillation ω using the concept of mutual inductance. The oscillating conducting ball sets up an emf in one coil and this varying emf can be recorded on an oscilloscope.

C. CONCLUSIONS

This thesis reports the design and construction of an acoustic chamber. Experimental tests show that the chamber is operating as designed. A homogeneous and isotropic acoustic field with an average total acoustic power of 133 dB can be produced inside the chamber. Initial acoustic analog

experiments for the Casimir force were conducted using Styrofoam plates and showed that the restoring effects of gravity prevented visual detection of the Casimir effect.

The acoustic chamber provides a valuable tool in understanding the effects of ZPF. The return on the investment of about \$300 (cost of buying raw materials used in building the chamber and experiments and 50 tweeters) is significant. Other experiments, regardless of whether or not they are related to Casimir Acoustics, can be performed. Design changes can be easily incorporated to tailor specific experiments.

It is the hope of the author that this acoustic chamber will spark some interest in this new area of basic research called Casimir acoustics.

LIST OF REFERENCES

- T. Boyer, 1969. "Derivation of the blackbody radiation without quantum assumptions," *Phys. Rev.* **182**, 1374-1383.
- H. B. G. Casimir, 1948. "On the attraction between two perfectly conducting plates," *Proc. Kon. Ned. Akad. Wetensch.* **51**, 793-796.
- H. B. G. Casimir and D. Polder, 1948. "The influence of retardation on the London-van der Waals forces," *Phys. Rev.* **73**, 360-372.
- C. Eberlein, 1996. "Theory of quantum radiation observed as sonoluminescence," *Phys. Rev. A* **53**, 2772-2787.
- B. Haisch, A. Rueda, and H. E. Puthoff, 1994. "Inertia as a zero-point-field Lorentz force," *Phys. Rev. A* **49**, 678-694.
- A. Larraza 1996. Private communication.
- E. M Lifshitz, 1956 "The theory of molecular forces between solids," *Sov. Phys. JETP* **2**, 73-83.
- J. J. Sakurai, 1967. *Advanced quantum mechanics* (Addison-Wesley, London), Secs. 2-4. and 2-8.

- J. Schwinger, "Casimir light: The source, 1993. " *Proc. Natl. Acad. Sci.* **90**, 2105-2106 .
- J. Schwinger, L. DeRaad, and K. A. Milton, 1978. "Casimir effect in dielectrics," *Ann. Phys.* **115**, 1-23.
- M. J., Sparnaay, 1958. "Measurements of attractive forces between flat plates," *Physica* **24**, 751-764.
- C. I. Sukenik, M. G. Boshier, D. Cho, V. Sandoghdar, and E. A. Hinds, 1993. "Measurements of the Casimir-Polder force," *Phys. Rev. Lett.* **70**, 560-563.

INITIAL DISTRIBUTION LIST

1. Defense Technical Information Center.....2
8725 John J. Kingman Rd., STE 0944
Ft. Belvoir, Virginia 22060-6218
2. Dudley Knox Library.....2
Naval Postgraduate School
411 Dyer Rd.
Monterey, California 93943-5101
3. Dr. William B. Colson, Code PH/Cw.....1
Department of Physics
Naval Postgraduate School
Monterey, California 93943-5002
4. Professor A. Larraza, Code PH/La.....2
Department of Physics
Naval Postgraduate School
Monterey, California 93943-5002
5. Professor B. Denardo.....2
National Center for Physical Acoustics
University of Mississippi
One Coliseum Drive
University, MS 38677
6. LCDR Robert T. Susbilla.....2
1254 Acadia Ave
Milpitas, CA 95035